C. R. Mecanique 341 (2013) 483–489

Contents lists available at SciVerse ScienceDirect

Comptes Rendus Mecanique

www.sciencedirect.com

10th International Meeting on Thermodiffusion

Stability of the advective flow of a binary mixture in a horizontal layer with adiabatic boundaries

Tatyana P. Lyubimova [a,b,*], Dmitriy V. Lyubimov [b], Dmitriy A. Nikitin [a], Anatolii V. Perminov [c]

[a] Institute of Continuous Media Mechanics UB RAS, 1, Koroleva Str., 614013, Perm, Russia
[b] Perm State National Research University, 15, Bukireva Str., 614990, Perm, Russia
[c] Perm National Research Polytechnic University, 29a, Komsomolsky Prosp., 614990, Perm, Russia

ARTICLE INFO

Article history:
Available online 27 February 2013

Keywords:
Binary fluid
Horizontal layer
Horizontal temperature gradient
Linear stability
Soret effect

ABSTRACT

Stability and nonlinear regimes of stationary advective flows of binary fluids in a horizontal layer subjected to a homogeneous longitudinal temperature gradient are studied for the case of rigid adiabatic boundaries. The problem is considered taking into account the Soret effect. Stability maps in the parameter plane "Rayleigh number–separation ratio" are obtained for several typical binary fluids.

© 2013 Académie des sciences. Published by Elsevier Masson SAS. All rights reserved.

1. Introduction

This paper is devoted to the investigation of stability and nonlinear spatially periodic regimes of advective flows of binary fluids in a horizontal layer with rigid adiabatic boundaries, taking into account the Soret effect.

There are a large number of papers devoted to the investigation of one- and two-dimensional advective flows of single-component fluids in a horizontal layer and horizontal rectangular enclosure for different thermal boundary conditions. Stability of stationary advective flows of single-component fluid in a horizontal layer with rigid boundaries was investigated in [1,2] for perfectly conductive boundaries (see also monograph [3]) and in [4] for insulated boundaries. Numerical investigation of stationary advective flows of single-component fluid in a horizontally elongated rectangular cavity with perfectly conductive and adiabatic boundaries was carried out in [5,6]. Stability of a binary fluid advective flow in a horizontal layer with rigid boundaries subjected to the homogeneous longitudinal temperature and concentration gradients was studied in [7]. The stationary advective flows of binary fluid in a horizontally elongated rectangular cavity with insulated boundaries were studied analytically and numerically in [8], taking into account the thermal diffusion and diffusive conductivity. The stability of the Soret-driven stationary advective flows of binary fluid in a horizontal layer with perfectly conductive boundaries subjected to the homogeneous longitudinal temperature gradient was studied in a recent paper [9]. The stability of stationary advective flows of binary fluid in a horizontal layer with adiabatic boundaries had not been considered earlier.

2. Problem formulation. Governing equations

Let us consider a binary fluid flow in a horizontal layer subjected to the homogeneous horizontal temperature gradient by setting different constant temperatures on the removed vertical walls and bounded at its top and bottom by rigid adiabatic plates $x = \pm h$ (x is the vertical axis and z is the horizontal axis along the layer). The fluid density is linearly dependent

* Corresponding author at: Institute of Continuous Media Mechanics UB RAS, 1, Koroleva Str., 614013, Perm, Russia.
E-mail address: lubimova@psu.ru (T.P. Lyubimova).

1631-0721/$ – see front matter © 2013 Académie des sciences. Published by Elsevier Masson SAS. All rights reserved.
http://dx.doi.org/10.1016/j.crme.2013.02.002

on the temperature and concentration of the lighter component $\rho = \langle\rho\rangle(1 - \beta_1 T - \beta_2 C)$, where $\langle\rho\rangle$ is the fluid density at some temperature and concentration values, which have been taken as the reference, T and C are the small deviations from these values, β_1 is the mixture thermal expansion coefficient, and β_2 is the concentration coefficient of density ($\beta_2 > 0$).

We choose the quantities h, h^2/χ, χ/h, Ah, $Ah\beta_1/\beta_2$ and $\langle\rho\rangle\nu\chi/h^2$ as the scales for length, time, velocity, temperature, concentration and pressure, respectively (A is the value of the imposed longitudinal temperature gradient).

The non-dimensional equations for buoyancy convection in the Boussinesq approximation accounting for the Soret effect (the effect of diffusive conductivity is assumed to be small) read:

$$\frac{1}{Pr}\left(\frac{\partial\vec{v}}{\partial t} + \vec{v}\cdot\nabla\vec{v}\right) = -\nabla p + \Delta\vec{v} + Ra(T + C)\vec{\gamma}, \quad \operatorname{div}\vec{v} = 0$$
$$\frac{\partial T}{\partial t} + \vec{v}\cdot\nabla T = \Delta T, \qquad \frac{\partial C}{\partial t} + \vec{v}\cdot\nabla C = \frac{1}{Le}(\Delta C - \varepsilon\Delta T) \tag{1}$$

Here $\vec{v}$ is the fluid velocity; p is the addition to the hydrostatic pressure due to convection; $\varepsilon = -\alpha\beta_2/\beta_1$ is the separation ratio; $Ra = g\beta_1 Ah^4/\nu\chi$ is the Rayleigh number; $Pr = \nu/\chi$ is the Prandtl number; $Le = \chi/D$ is the Lewis number; g is the gravity force acceleration; ν and χ are the kinematic viscosity and thermal diffusivity of the mixture, respectively; D is the diffusion coefficient; $\alpha = k_T/T_a$, where k_T is the thermodiffusion ratio, T_a is the absolute temperature; $\vec{\gamma}$ is the unit vector directed vertically upward. The temperature and concentration dependences of the parameter α and other kinetic coefficients are neglected.

On the layer boundaries, we set the no-slip conditions and the absence of heat and mass fluxes. In addition, the closeness conditions for the flow and solute flux associated with diffusion, thermodiffusion and convection are imposed. The value of the horizontal temperature gradient is assumed to be fixed:

$$\vec{v} = 0, \qquad \frac{\partial T}{\partial n} = 0, \qquad \frac{\partial C}{\partial n} + \varepsilon\frac{\partial T}{\partial n} = 0, \qquad \int \vec{v}\,dS = 0, \qquad \int (Le\,\vec{v}C - B + \varepsilon)\,dS = 0 \tag{2}$$

3. Basic solution

We search for the steady-state solution of the problem in the form:

$$\vec{v} = \big(0, 0, v_0(x)\big), \qquad C_0 = Bz + c_0(x), \qquad T_0 = z + \vartheta_0(x), \qquad p = p_0(x, z) \tag{3}$$

Here B is the longitudinal concentration gradient formed in the layer, the value of which is to be defined; v_0 is the basic state velocity directed along the z-axis.

The equations and boundary conditions describing the basic state (3) have the form:

$$\frac{\partial^3 v_0}{\partial x^3} = Ra(1 + B), \quad v_0 = \frac{\partial^2\vartheta_0}{\partial x^2}, \qquad -LeBv_0 = \frac{\partial^2 c_0}{\partial x^2} - \varepsilon\frac{\partial^2\vartheta_0}{\partial x^2} \tag{4}$$
$$x = \pm 1: \quad v_0 = 0, \quad \frac{\partial\vartheta_0}{\partial x} = 0, \quad \frac{\partial c_0}{\partial x} = 0 \tag{5}$$

and the closeness conditions for the flow and solute flux are:

$$\int_{-1}^{1} v_0\,dx = 0, \qquad \int_{-1}^{1} (Le\,v_0 c_0 - B + \varepsilon)\,dx = 0 \tag{6}$$

The problem (4)–(6) is nonlinear. By solving this problem, we obtain the following expressions for velocity, temperature and concentration profiles in a steady state:

$$v_0 = V_0 x\big(x^2 - 1\big), \qquad \vartheta_0 = \frac{1}{60}V_0 x\big(3x^4 - 10x^2 + 15\big), \qquad c_0 = (LeB + \varepsilon)\vartheta_0 \tag{7}$$

The value of the horizontal concentration gradient B is obtained from (6):

$$B = -\varepsilon\big(8V_0^2 Le - 315\big)/\big(8V_0^2 Le^2 + 315\big) \tag{8}$$

and the relation between the velocity amplitude V_0 and the Rayleigh number is given by the formula:

$$Ra = \frac{6V_0}{1 + B} = \frac{6V_0(8V_0^2 Le^2 + 315)}{8V_0^2 Le^2 + 315 - 8\varepsilon V_0^2 Le + 315\varepsilon} \tag{9}$$

For small values of the Rayleigh number and finite values of the Lewis number, we obtain, from (8) and (9):

$$V_0 = \frac{1}{6}(1 + \varepsilon)Ra + O\big(Ra^3\big), \qquad B = \varepsilon + O\big(Ra^2\big) \tag{10}$$

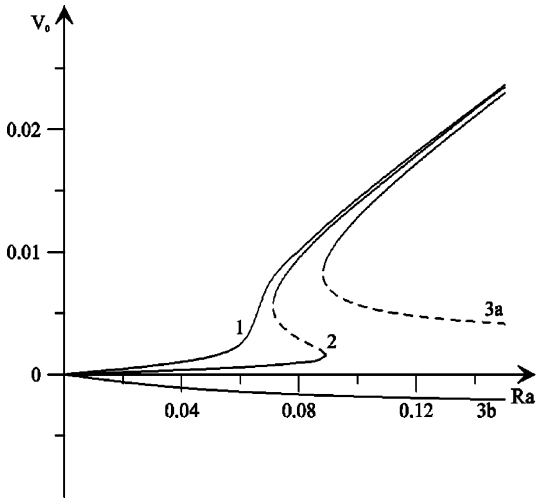

Fig. 1. Steady-state flow amplitude V_0 vs. Rayleigh number for $Pr = 0.01$, $Le = 1000$ and $\varepsilon = -0.87, -0.95, -1.2$ (curves 1–3).

In the case of the positive Soret effect ($\varepsilon > 0$), thermodiffusion results in the accumulation of the lighter component in the warmer part of the layer. Thus, when $\varepsilon > 0$ the fluid density near the hot boundary decreases, due to both thermal expansion and accumulation of the lighter component. As it is seen from (10), in this case the thermodiffusion leads to the convective flow velocity growth. In the case of the negative Soret effect ($\varepsilon < 0$), when thermodiffusion results in the accumulation of the lighter component in the colder part of the layer, the flow intensity decreases and, at $\varepsilon = -1$, the velocity takes a zero value together with the density gradient. Note that at $\varepsilon = -1$ the diffusive state may exist for any value of the Rayleigh number. At $\varepsilon < -1$, the velocity has the opposite sign due to the change in the sign of the density gradient.

The nonlinearity of the problem results in the possibility of the solution's non-uniqueness. It is possible to show that, for $\varepsilon > \varepsilon_* = -8Le/(9Le + 1)$, the solution is unique, and at $\varepsilon < \varepsilon_*$, there is an interval of the Rayleigh number (which is dependent on ε), in which there are three steady-state solutions. The boundaries of the domain of non-uniqueness correspond to the tangent bifurcation. They are obtained in the parametric form:

$$Ra = \frac{99\,225Le + 2520\xi^2(3Le + 1) - 64\xi^4}{840\xi Le(Le + 1)}, \qquad \varepsilon = -\frac{(8\xi^2 + 315)^2 Le}{99\,225Le + 2520\xi^2(3Le + 1) - 64\xi^4}$$

where $\xi = V_0 Le$.

For $\varepsilon > -1$, the domain of non-uniqueness is bounded from above and from below and exists at $\varepsilon < \varepsilon_*$, whereas for $\varepsilon \leqslant -1$ the domain of non-uniqueness is bounded only from below.

The case $\varepsilon = -1$ is special. For $\varepsilon = -1$, the diffusive state corresponds to one of the branches of the steady-state solution, in which the thermal and concentration effects compensate each other. For this special case, the interesting dynamics is obtained in [10] for the rectangular cavity with an aspect ratio equal to 2. In [11], the onset of double diffusive convection in vertical enclosures with equal and opposing buoyancy forces due to horizontal thermal and concentration gradients was studied. It is verified that the onset of double diffusive convection corresponds to a transcritical bifurcation point.

The diagram $V_0(Ra)$ for $Pr = 0.01$, $Le = 1000$ and $\varepsilon = -0.87, -0.95, -1.2$ (curves 1–3) is shown in Fig. 1, where the solid lines correspond to the stable branches of steady-state solutions and the dashed lines to the unstable branches.

4. Problem of the stability of basic state

Let us consider the stability of the basic state (7)–(9). Linearized equations and boundary conditions for small perturbations of the basic state have the form:

$$\frac{1}{Pr}\left(\frac{\partial \vec{v}}{\partial t} + \vec{v}\cdot\nabla\vec{v}_0 + \vec{v}_0\cdot\nabla\vec{v}\right) = -\nabla p + \Delta\vec{v} + Ra(T + C)\vec{\gamma}, \quad \operatorname{div}\vec{v} = 0$$
$$\frac{\partial T}{\partial t} + \vec{v}\cdot\nabla T_0 + \vec{v}_0\cdot\nabla T = \Delta T, \qquad \frac{\partial C}{\partial t} + \vec{v}\cdot\nabla C_0 + \vec{v}_0\cdot\nabla C = \frac{1}{Le}(\Delta C - \varepsilon\Delta T)$$
$$x = \pm 1: \quad \vec{v} = 0, \quad \frac{\partial T}{\partial x} = 0, \quad \frac{\partial C}{\partial x} = 0 \tag{11}$$

In the general case of three-dimensional perturbations, all quantities are proportional to $\exp[-\lambda t + i(k_y y + k_z z)]$ (here the y-axis is the horizontal axis perpendicular to the direction of the basic flow). For the problem under consideration, there

is no analogue of the Squire transformation, i.e. no transformation, which reduces the three-dimensional problem to the two-dimensional one. For that reason, two limit cases were considered: plane perturbations with $k_y = 0$ (the rolls with axes perpendicular to the basic flow direction), and spiral perturbations with $k_z = 0$ (the rolls with axes parallel to the basic flow direction).

5. Long-wave instability of a steady-state unidirectional flow

It is impossible to obtain the analytical solution of the stability problem (11) for arbitrary values of the wave number. However, the case of long-wave perturbations allows full enough analytical investigation. For that, the solution of the problem and the increment were represented in the form of power series in wave number.

For plane long-wave perturbations, the stability boundaries in the parameter plane Ra–ε are obtained under the form:

$$Ra = \frac{6\xi(8\xi^2 + 315)}{8\xi^2(Le - \varepsilon) + 315Le(\varepsilon + 1)}$$

$$\varepsilon = \frac{Le(8\xi^2 + 105Le^2)(8\xi^2 + 315)^2}{512\xi^6 + 6720(Le^2 - 5Le + 1)(\xi^4 - 264\,600Le(3Le^2 + Le + 3)\xi^2 - 10\,418\,625Le^3)}$$

and, for spiral perturbations, under the form:

$$Ra = \frac{6\xi(8\xi^2 + 315)}{8\xi^2(Le - \varepsilon) + 315Le(\varepsilon + 1)}, \qquad \varepsilon = -\frac{(8\xi^2 + 315)(12\xi^2 + 8\,Pr\,\xi^2 + 315Le^2Pr)}{64\,Pr\,\xi^4 + 3780\xi^2(Le + 1) + 2520\,Pr\,\xi^2(Le^2 + 1)}$$

6. Instability to perturbations with finite wave numbers

The instability to the perturbations with finite wave numbers was investigated numerically by solving the boundary-value problems for small normal-mode perturbations by the collocation method. The Chebyshev polynomials were used as the trial functions. The number of trial functions was chosen from the requirement of convergence of the results and was varied from 15 to 30 for different instability modes.

For single-component fluid, the instability of the unidirectional steady advective flow in a plane horizontal layer with adiabatic boundaries may occur due to the plane monotonous hydrodynamic mode associated with the development of stationary vortices at the boundary of towards flows, spiral oscillatory mode related to the excitation of internal waves in the zone of stable stratification, and spiral monotonous mode [4]. The hydrodynamic mode is the most dangerous at small values of the Prandtl number $0 < Pr < 0.033$, at $Pr \approx 0.12$ this instability mode is strongly stabilized due to the formation of stable temperature stratification in the zone of vortex formation. In the range $0.033 < Pr < 0.2$ the spiral oscillatory mode is the most dangerous. At $Pr \approx 0.25$, this mode is also sharply stabilized and the spiral monotonous mode, lying at small Prandtl numbers much higher than the first two modes, becomes the most dangerous.

In the present paper, we consider three typical binary mixtures: 1, the liquid metal mixture with $Pr = 0.01$, $Le = 1000$ (hereinafter, mixture 1); 2, the gaseous mixture with $Pr = 0.7$, $Le = 13/7$ (hereinafter, mixture 2); 3, the solution of salt in water with $Pr = 6.7$, $Le = 101$ (hereinafter, mixture 3).

In Figs. 2–4, the stability maps of the advective flow in the parameter plane Ra–ε are plotted for mixtures 1–3. The domains of instability of the upper branch of stationary solutions are shown by shading to the left and the domains of instability of the lower branch – by shading to the right, the double shading corresponds to the domains of the parameter values in which all branches of stationary solutions are unstable. The structure of critical perturbations, corresponding to different instability modes, is also shown in these figures.

In Fig. 2, the stability map for mixture 1 is plotted. For this mixture, the stationary advective flow is unique at $\varepsilon > -0.88$ and there are three stationary solutions at $\varepsilon < -0.88$. Curve 1, which intersects the axis $\varepsilon = 0$ at $Ra = 5.103$, corresponds to the hydrodynamic instability mode with $k \approx 1.3$; curve 2, intersecting the axis $\varepsilon = 0$ at $Ra = 10.28$, to the large-scale spiral oscillatory perturbations with $k \approx 0.22$, $\omega \approx 8.9$; curve 3, which intersects the axis $\varepsilon = 0$ at $Ra = 181.1$, to the monotonous spiral instability mode with $k \approx 2.9$. As one can see, at $\varepsilon > -0.88$ the thermodiffusion has practically no effect on the occurrence of instability of basic flow of the mixture 1, all three curves are nearly horizontal, i.e. the behavior of the mixture is close to that of a single-component fluid. The only difference is that the monotonous spiral mode (curve 3) at $\varepsilon \approx 0.4$ becomes oscillatory; besides, the critical Rayleigh number remains nearly the same and the oscillation frequency varies from $\omega \approx 0.27$ to $\omega \approx 1.3$.

At $\varepsilon < -0.88$, the stationary solution of mixture 1 is non-unique. The boundaries of non-uniqueness are shown in Fig. 2 by dash-dotted lines 4, 4′. In the range of ε values from -0.88 to -1, the non-uniqueness domain is bounded both from above and below. At $\varepsilon = -1$ for the lower branch of stationary solutions, the velocity is zero and at $\varepsilon < -1$, it is of the opposite sign; moreover, this branch exists for any values of the Rayleigh number. When the Rayleigh number $Ra_*(\varepsilon)$ corresponds to curve 4, two upper branches of solutions are born through a tangent bifurcation; they exist at any $Ra > Ra_*(\varepsilon)$.

At $\varepsilon < -0.88$ the effect of thermodiffusion is significant. The instability boundaries 1, 2, 3 discussed above remain nearly horizontal as in the case when $\varepsilon > -0.88$. However, at $\varepsilon < -0.88$, there exists much more dangerous instability mode; it is

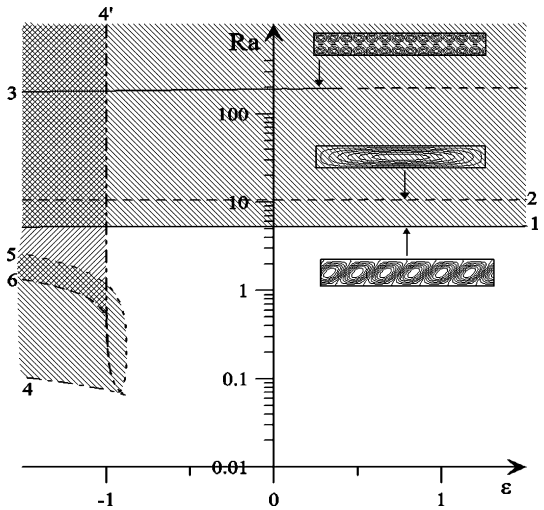

Fig. 2. Boundaries of the domain of non-uniqueness of the stationary solution (dash-dotted lines 4, 4′) and instability boundaries for mixture 1 ($Pr = 0.01$, $Le = 1000$): curves 1–3, 5 for the upper branch of stationary solutions, curve 6 for the lower branch; 1, plane cellular monotonous hydrodynamic mode; 2, spiral cellular oscillatory mode; 3, spiral cellular mode; dash-dotted line 5, long-wave spiral monotonous mode; 6, plane cellular mode. Streamlines for different instability modes.

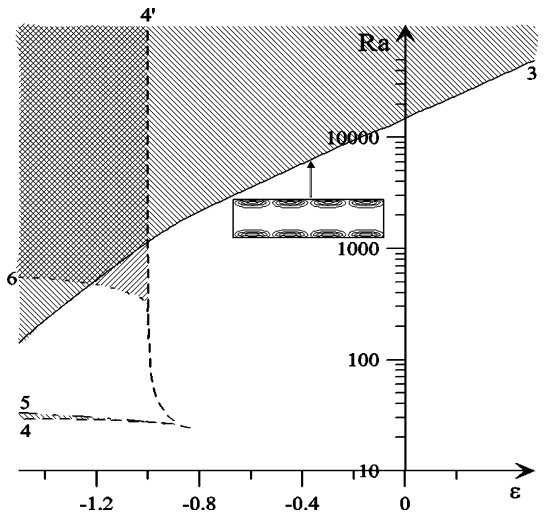

Fig. 3. Boundaries of the domain of non-uniqueness of the stationary solution (dash-dotted lines 4, 4′) and instability boundaries for mixture 2 ($Pr = 0.7$, $Le = 13/7$). Notations are the same as in Fig. 1. Streamlines of critical perturbations for spiral monotonous cellular mode.

the long-wave spiral monotonous mode, which is related to the effect of thermodiffusion and is absent in the case of a single-component fluid.

The instability domain at $\varepsilon < -0.88$ lies between curves 5 and 4. At the lower boundary of this domain, the instability to the perturbations in the whole range of wave number values (from zero to some finite value) exists. With the increase of the Rayleigh number, the range of wave numbers corresponding to the growing perturbations is reduced and, at the upper boundary, the instability exists only for long-wave perturbations. The middle branch of stationary solutions is always unstable in the domain of non-uniqueness, and the lower branch corresponds to unstable plane cellular perturbations above curve 6.

Let us now discuss the results for mixture 2. In the case of a single-component fluid at $Pr = 0.7$, the instability of stationary advective flow is associated with the development of spiral monotonous perturbations with a wave number close to 2 [4] (hydrodynamic and spiral oscillatory modes are subjected to sharp stabilization at lower Prandtl number values and at $Pr = 0.7$ they are absent). Curve 3 in Fig. 3, defining the instability boundary to spiral monotonous perturbations for mixture 2, crosses the axis $\varepsilon = 0$ at $Ra = 14834$. For the positive Soret effect, this instability mode is strongly stabilized, whereas for the negative Soret effect, it is strongly destabilized. The structure of the critical perturbation corresponding to this mode is also shown in Fig. 3.

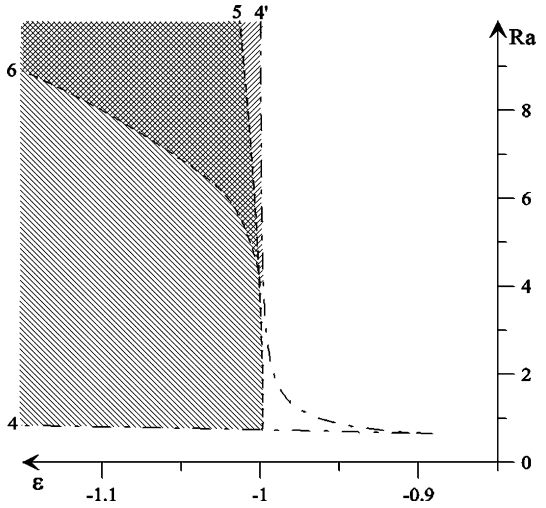

Fig. 4. Instability boundaries for mixture 3 ($Pr = 6.7$, $Le = 101$): solid lines, instability boundaries of the upper branch of stationary solutions to the long-wave plane monotonous mode; dash-dotted lines, to the long-wave spiral monotonous mode; curve 6, lower instability boundary for the lower branch of stationary solutions.

The spiral monotonous perturbations with finite wave numbers are most dangerous at $\varepsilon > -0.84$. In the narrow range of values of the separation ratio $-0.85 < \varepsilon < -0.84$, the instability occurs due to long-wave spiral perturbations and, at $\varepsilon < -0.85$, instability to spiral perturbations in the whole range of wave number values (from zero to some finite value) takes place. As in the case of mixture 1, for negative ε sufficiently large in absolute value, there exists an instability domain of the upper branch of stationary solutions to spiral monotonous perturbations with small wave numbers. Conversely, unlike in the case of mixture 1, this domain, confined between curves 4 and 5, is rather narrow.

As well as for the mixture 1, the lower branch of stationary solutions is unstable to the plane perturbations above curve 6.

At $Pr = 6.7$, the stationary advective flow of the single-component fluid is stable [4]. The positive Soret effect does not lead to the appearance of instability. For the negative Soret effect in the domain of non-uniqueness of stationary flow, as in the cases discussed above, the upper branch of stationary solutions is unstable to the long-wave spiral perturbations in the parameter range which corresponds to the domain between curves 4 and 5 in Fig. 4; the lower branch is unstable above curve 6.

7. Nonlinear regimes

Investigation of nonlinear regimes of advective flows of binary mixtures was carried out numerically. The calculations were performed following a two-dimensional approach. Applying the operation rot_y to the first equation of (1), introducing the stream function ψ and the vorticity φ as $\vec{v} = rot(\psi \vec{j})$, $rot_y \vec{v} = -\Delta\psi = \varphi$ and separating the linear horizontal distributions of temperature and concentration $T = \vartheta + z$, $C = c + Bz$, where B is calculated from the formula (7), we obtain the following system of equations and boundary conditions at the horizontal boundaries:

$$\begin{aligned}
&\frac{\partial\varphi}{\partial t} = \Delta\varphi + Ra\left[1 + B + \frac{\partial}{\partial z}(\vartheta + c)\right] + \frac{1}{Pr}\left(\frac{\partial\psi}{\partial z}\frac{\partial\varphi}{\partial x} - \frac{\partial\psi}{\partial x}\frac{\partial\varphi}{\partial z}\right), \quad \Delta\psi = -\varphi\\
&\frac{\partial\vartheta}{\partial t} = \frac{1}{Pr}\left(\Delta\vartheta + \left(\frac{\partial\psi}{\partial z}\frac{\partial\vartheta}{\partial x} - \frac{\partial\psi}{\partial x}\frac{\partial\vartheta}{\partial z}\right) - \frac{\partial\psi}{\partial x}\right)\\
&\frac{\partial c}{\partial t} = \frac{1}{Le\,Pr}(\Delta c - \varepsilon\Delta\vartheta) + \frac{1}{Pr}\left(\left(\frac{\partial\psi}{\partial z}\frac{\partial c}{\partial x} - \frac{\partial\psi}{\partial x}\frac{\partial c}{\partial z}\right) - B\frac{\partial\psi}{\partial x}\right)\\
&x = \pm 1: \quad \psi = \frac{\partial\psi}{\partial x} = 0, \quad \frac{\partial\vartheta}{\partial x} = \frac{\partial c}{\partial x} = 0
\end{aligned} \tag{12}$$

On vertical boundaries of the cell, the periodicity conditions were imposed for ψ, φ, ϑ, c.

The problem (12) was solved by the finite difference method. The central differences were used for approximating spatial derivatives. The Poisson equation at each time step was solved by successive iterations of the over-relaxation method. The calculations were performed for the cell of plane horizontal layer whose length was taken equal to the wavelength of the most dangerous perturbations according to the results of the linear stability analysis. Periodicity conditions were imposed at the vertical boundaries of the cell. We used the uniform mesh with square cells. The mesh size in the main calculations

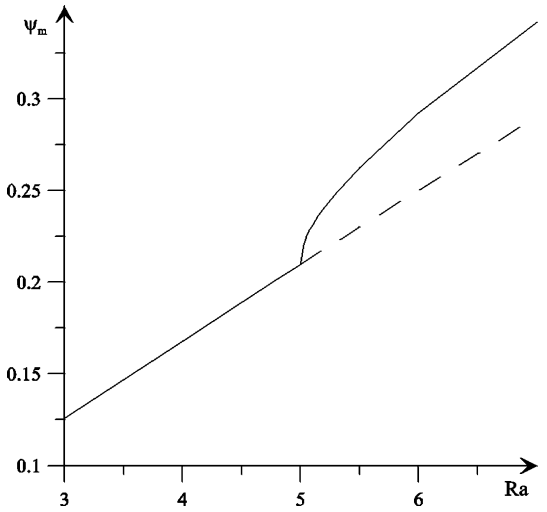

Fig. 5. Dependence of the maximal value of the stream function of the Rayleigh number for stationary flows at $Pr = 0.01$, $Le = 1000$, $\varepsilon = -0.5$.

was taken to be 1/30 (this step was chosen on the basis of the results of test calculations performed with different mesh sizes, and to control the convergence of the results with the mesh refinement).

In Fig. 5, the dependence of the maximal value of the stream function in the cavity on the Rayleigh number is shown for stationary flows at $Pr = 0.01$, $Le = 1000$, $\varepsilon = -0.5$. According to the results of the linear stability analysis, the stationary advective flow becomes unstable, for these parameter values, to plane monotonous cellular hydrodynamic perturbations at $Ra = Ra_{\mathrm{cm}} \approx 5.09$ (see Fig. 2, curve 1). As seen in Fig. 5, the results of nonlinear calculations agree well with the results of linear stability analysis: at values of the Rayleigh number smaller than Ra_{cm}, the dependence $\psi_{\mathrm{m}}(Ra)$ is nearly linear and at $Ra \approx Ra_{\mathrm{cm}}$ a new solution branches from this line with a square-root law.

8. Conclusions

The calculations carried out for three different binary mixtures showed that, for the positive Soret effect, $\varepsilon > 0$ at small values of the Prandtl number and large values of the Lewis number, which is typical of liquid metal binary melts, whereas the effect of thermodiffusion on the stability of a steady flow is weak, and that, at Lewis and Prandtl number values of the order of unity, thermodiffusion has a significant stabilizing effect. In all considered cases, thermodiffusion leads to non-uniqueness of the stationary solution. There is the range of ε values where the three branches of stationary solutions exist simultaneously. For the upper branch of stationary solutions, there is instability to the same modes as in the case of the positive Soret effect; however, the most dangerous is the long-wave monotonous spiral mode, the origin of which is associated with thermodiffusion. The middle branch of stationary solutions is always unstable and the lower branch is unstable at $\varepsilon < -1$ and Rayleigh number values lower that certain critical value Ra_{cm}. The numerical solution of the full nonlinear problem shows that, for Rayleigh number values less than Ra_{cm}, the dependence of the maximal value of the stream function on the Rayleigh number is close to linear, and at $Ra \approx Ra_{\mathrm{cm}}$ a new solution branches from this line with a square-root law.

References

[1] G.Z. Gershuni, E.M. Zhukhovitskii, V.M. Myznikov, Stability of a plane-parallel convective flow of a liquid in a horizontal layer, J. Appl. Mech. Tech. Phys. 15 (1974) 78–82.
[2] G.Z. Gershuni, E.M. Zhukhovitskii, V.M. Myznikov, Stability of plane-parallel convective fluid flow in a horizontal layer relative to spatial perturbations, J. Appl. Mech. Tech. Phys. 15 (1974) 706–708.
[3] G.Z. Gershuni, E.M. Zhukhovitskii, A.A. Nepomnyashchy, Stability of Convective Flows, Nauka, Moscow, 1989.
[4] H.P. Kuo, S.A. Korpela, Stability and finite amplitude natural convection in a shallow cavity with insulated top and bottom and heated from a side, Phys. Fluids 31 (1988) 33–42.
[5] J.E. Drummond, S.A. Korpela, Natural convection in a shallow cavity, J. Fluid Mech. 182 (1987) 543–564.
[6] A.Yu. Gelfgat, P.Z. Bar-Yoseph, A.L. Yarin, Stability of multiple steady states of convection in laterally heated cavities, J. Fluid Mech. 388 (1999) 315–334.
[7] G.Z. Gershuni, A.V. Shalimov, V.M. Myznikov, Plane-parallel advective binary mixture flow stability in a horizontal layer, Int. J. Heat Mass Transfer 37 (1994) 2327–2342.
[8] M. Ouriemi, P. Vasseur, A. Bahloul, L. Robillard, Natural convection in a horizontal layer of a binary mixture, Int. J. Thermal Sci. 45 (2006) 752–759.
[9] D.V. Lyubimov, T.P. Lyubimova, D.A. Nikitin, A.V. Perminov, Stability of a binary-mixture advective flow in a plane horizontal layer with perfectly heat conducting boundaries, Fluid Dyn. 45 (2010) 458–467.
[10] E. Meca, I. Mercader, O. Batiste, L. Ramirez-Piscina, Complex dynamics in double-diffusive convection, Theor. Comput. Fluid Dyn. 18 (2004) 231–238.
[11] K. Ghorayeb, A. Mojtabi, Double diffusive convection in a vertical rectangular cavity, Phys. Fluids 9 (1997) 2339–2348.